Automatic anisotropic migration velocity analysis for reverse-time migration

Wiktor Weibull, NTNU, Børge Arntsen, NTNU, Marianne Houbiers, Statoil ASA and Joachim Mispel, Statoil ASA*

SUMMARY

The need for accurate seismic images over complex geological settings has driven the development of modern prestack depth migration algorithms, such as wave equation migration (WEM) and reverse-time migration (RTM). These algorithms can cope not only with strong and sharp seismic velocity variations, but also with the complication of anisotropy. However, the imaging results still rely strongly on the quality of the velocity model estimation. In this paper we implement an automatic velocity analysis method based on focusing of anisotropic RTM of surface seismic data. The proposed method can deal with any form of anisotropy, but in this paper we focus on a vertically transverse isotropic medium (VTI). By assuming a fixed ratio between the anisotropic parameters, the number of parameters to be estimated is reduced to two. The method is tested on 2D synthetic and real field datasets. In both cases the velocity analysis produce well focused images. However, the results of the synthetic data example show that the method is relatively insensitive to the anisotropic parameters.

INTRODUCTION

Seismic imaging over complicated geological environments demands sofisticated depth migration algorithms, capable of accurately dealing with large lateral variations in velocity and with anisotropy. Perhaps, equally important to the need for accurate imaging methods is the need for better velocity estimation methods. Ideally, the velocity analysis method and the depth migration algorithm should be based on the same solution to the wave equation. This ideal has motivated the development of a series of velocity analysis methods, commonly grouped under the name of wave equation migration velocity analysis (WEMVA) (Sava and Biondi, 2004). As the name implies these techniques attempt to estimate seismic velocities through the focusing of depth migrated seismic data. The approach is based on formulating an objective function that measures to what extent subsurface offset- or angle-gathers are focused or flattened respectively, and then minimizing the objective function with respect to the velocity field.

A major strength of WEMVA is that it can be made fully automatic, and uses all events present in the seismic image to constrain the velocity model. Also by proper choice of the objective function, the method is less sensitive to the cycle skipping problems common to waveform fitting methods such as full waveform inversion (Tarantola, 1984; Symes and Carazzone, 1991). This makes WEMVA a robust method that can be applied in areas where the prior information is vague or nonexistent.

Most implementations of WEMVA are based on the acoustic isotropic approximation. One reason for this is that this approximation usually produces a satisfactory result. Another reason is that, under an acoustic isotropic medium, the velocity field can be described by a single spatially varying parameter, the P-wave velocity. Whereas for an anisotropic medium there are at least three parameters that need to be estimated. However, in cases where the velocity field is anisotropic, velocity analysis under an isotropic assumption will lead to an inaccurate solution.

In this paper we investigate whether it is possible to use WEMVA to estimate one additional anisotropic parameter from surface seismic data. For this purpose we propose a WEMVA method based on a combination of the similarity-index (Chavent and Jacewitz, 1995), differential semblance (Symes and Carazzone, 1991) and anisotropic RTM. We choose to use RTM because this method provides an accurate solution to the wave propagation problem, in particular at large angles, which are crucial for anisotropic parameter estimation.

In the next section, we present the basic equations we used to set up the optimization problem. Then we show the results of both a 2D synthetic and real field data example, which confirm the viability of the method.

THEORY

The theory for reverse time migration is founded on nonlinear inversion theory (Tarantola, 2005). Depth images are produced by crosscorrelating a source wavefield forward propagated in time with a residual wavefield backward extrapolated in time. In the context of full waveform inversion, these images represent the gradients of the least square misfit function with respect to the material parameters. On the other hand, if the residual wavefield is given by the single scattering recorded data, we obtain Claerbout's imaging condition (Claerbout, 1971). According to this condition, given an accurate estimate of the material velocities, the crosscorrelation of the reconstructed source and receiver wavefields will have a maximum at zero lag in time and space. In Differential Semblance optimization, this fact is explored to set up a non-linear least squares inversion problem (Symes and Carazzone, 1991). By parametrizing the image with an additional lag parameter it is possible to capture the deviation of the maximum in crosscorrelation from zero lag (Rickett and Sava, 2002). The resultant image volume can then be used to quantify the error in the estimates of the velocities (Shen and Symes, 2008).

In this paper we use an RTM image (R) parametrized by horizontal spatial lag ($\mathbf{h}$) :

$$R(\mathbf{x},\mathbf{h}) = \sum_s \int_0^T dt \; \frac{\partial u_i^{fw}}{\partial x_i}(\mathbf{x}-\mathbf{h},t,s)\frac{\partial u_j^{bw}}{\partial x_j}(\mathbf{x}+\mathbf{h},t,s),$$

where $i,j = x,z$ are indexes under Einstein summation convention, $\mathbf{x} = (x,z)$ are the spatial coordinates, $\mathbf{h} = (h_x,0)$ is

the subsurface horizontal half-offset, t is the time and s is the source index.

The wavefields u_i^{fw} and u_i^{bw} are the reconstructed source and receiver displacement wavefields, respectively. These wavefields are computed by solving the following modeling equations:

$$u_i^{fw}(\mathbf{x},t,s) = \int d\mathbf{x}'\, G_{ij}(\mathbf{x},t;\mathbf{x}',0) * \delta(\mathbf{x}'-\mathbf{x}_s)\frac{\partial S}{\partial x'_j}(\mathbf{x}',t,s)$$

$$u_i^{bw}(\mathbf{x},t,s) = \int d\mathbf{x}'\, G_{ij}(\mathbf{x},0;\mathbf{x}',t) * \sum_{r=1}^{Nr}\delta(\mathbf{x}'-\mathbf{x}_r)\frac{\partial P}{\partial x'_j}(\mathbf{x}',-t,s)$$

Where G_{ij} is the constant density elastic Green's function, $*$ denotes time convolution, S is the pressure source function, P is the recorded pressure data, r is the receiver index, and δ is the Kroenecker delta.

Anisotropy

To model the kinematics of wave propagation over an anisotropic medium, we use a constant density elastic wave equation. Different from other anisotropic wave equations, such as the acoustic approximation of Alkhalifah (2000), our implementation is stable under any form of physically realizable variation of material properties. The constant density elastic wave equation can be written as (Ikelle and Amundsen, 2005):

$$\frac{\partial^2 u_i}{\partial t^2}(\mathbf{x},t) - \frac{\partial}{\partial x_j}\left[v_{ijkl}(\mathbf{x})\frac{\partial u_l}{\partial x_k}(\mathbf{x},t)\right] = F_i(\mathbf{x},t)$$

where u_i is the displacement vector, v_{ijkl} is a velocity tensor, and F_i is a source term.

In a general anisotropic medium, v_{ijkl} contains 21 independent parameters. However, in this paper we only estimate 2 parameters. We assume a VTI medium with constant S-wave velocity and fixed ratio between the Thomsen's parameters ε and δ (Thomsen, 1986). The coupling of the anisotropic parameters is an attempt to increase the sensitivity to anisotropy and reduce the number of parameters to be estimated. This way, v_{ijkl} can be fully described by the P-wave velocity along the symmetry axis (V_{P0}) and one anisotropic parameter (coupling between Thomsen's ε and δ).

Velocity analysis

The velocity analysis is based on non-linear optimization of the following objective function:

$$J = DS - SI. \tag{1}$$

The objective function is composed of two parts, the differential semblance misfit (DS) and the similarity-index (SI).

The differential semblance misfit quantifies the deviation of the image from focus, and is given by (Weibull and Arntsen, 2011):

$$DS = \frac{1}{2}\left\|\mathbf{h}\frac{\partial R}{\partial z}(\mathbf{x},\mathbf{h})\right\|^2 \tag{2}$$

The similarity-index measures the stack quality of the image. It is very nonlinear, but has a strong peak at the correct background velocities and helps to prevent the amplitude dimming related to artifacts in the solution of the differential semblance optimization (Shen and Symes, 2008):

$$SI = \frac{\gamma}{2}\left\|\frac{\partial R}{\partial z}(\mathbf{x},\mathbf{h}=0)\right\|^2 \tag{3}$$

where γ is a constant which balances the weight of SI over DS. Ideally, it should be set such that SI only acts as a regularization.

The errors quantified by the objective function (J) can be turned into velocity updates by a non-linear iterative optimization process. In this process, it is necessary to compute the gradients of the misfit function with respect to the velocity parameters.

The gradients can be computed in a similar fashion to the depth migration described above, by the adjoint state method (Chavent, 2009):

$$\nabla_{\mathbf{m}} J(\mathbf{x}) = \sum_s \int dt \frac{\partial v_{ijkl}}{\partial \mathbf{m}}(\mathbf{x})\frac{\partial u_l^{fw}}{\partial x_k}(\mathbf{x},t,s)\frac{\partial \psi_i^{fw}}{\partial x_j}(\mathbf{x},t,s) + \sum_s \int dt \frac{\partial v_{ijkl}}{\partial \mathbf{m}}(\mathbf{x})\frac{\partial u_l^{bw}}{\partial x_k}(\mathbf{x},t,s)\frac{\partial \psi_i^{bw}}{\partial x_j}(\mathbf{x},t,s)$$

where $\mathbf{m} = [V_{P0}(\mathbf{x}), \varepsilon(\mathbf{x}), \delta(\mathbf{x}) = k\varepsilon(\mathbf{x})]$, and k is a constant that couples Thomsens's ε and δ.

The wavefields ψ_i^{fw} and ψ_i^{bw} are adjoint states that can be computed by the following adjoint modelings:

$$\psi_i^{fw}(\mathbf{x},t,s) = \int d\mathbf{x}' \frac{\partial G_{ij}}{\partial x'_j}(\mathbf{x},0;\mathbf{x}',t) * F_D(\mathbf{x}',t,s),$$

and

$$\psi_i^{bw}(\mathbf{x},t,s) = \int d\mathbf{x}' \frac{\partial G_{ij}}{\partial x'_j}(\mathbf{x},t;\mathbf{x}',0) * F_U(\mathbf{x}',t,s).$$

Here F_D and F_U are residual sources given by:

$$F_D(\mathbf{x}',t,s) = \int d\mathbf{h}\,(\mathbf{h}^2 - \delta(\mathbf{h})\gamma)\frac{\partial^2 R}{\partial z'^2}(\mathbf{x}'+\mathbf{h},\mathbf{h})\frac{\partial u_l^{bw}}{\partial x'_l}(\mathbf{x}'+2\mathbf{h},t,s),$$

and

$$F_U(\mathbf{x}',t,s) = \int d\mathbf{h}\,(\mathbf{h}^2 - \delta(\mathbf{h})\gamma)\frac{\partial^2 R}{\partial z'^2}(\mathbf{x}'-\mathbf{h},\mathbf{h})\frac{\partial u_l^{fw}}{\partial x'_l}(\mathbf{x}'-2\mathbf{h},t,s).$$

RESULTS AND DISCUSSION

Synthetic data example

The synthetic velocity model used in the first example is shown in figure 1. The model is a 2D synthetic cross section of the Snorre field offshore Norway. The anisotropic model simulates a medium with both elliptical ($\varepsilon = \delta$) and anelliptical VTI layers. This model was used to generate synthetic seismic

data using a finite difference solution to the elastic wave equation (Lisitsa and Vishnevskiy, 2010). The geometry of the data consists of a line with minimum offset of 150 meters and maximum offset of 6 kilometers. Absorbing boundary conditions were used to ensure that the data is free from surface related multiples. However, interbeded multiples and converted waves are still present in the data.

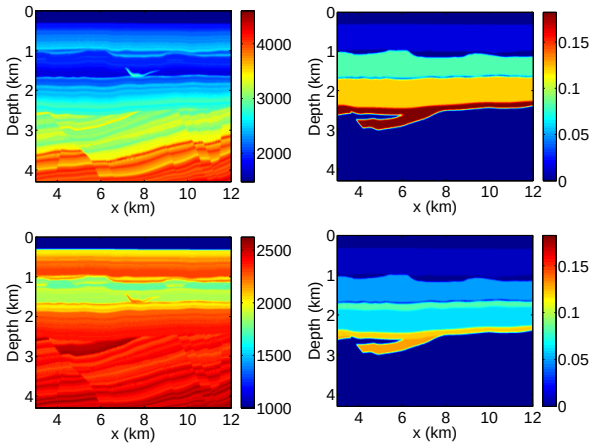

Figure 1: Synthetic anisotropic model; Left: V_{P0} (top); Density (bottom). Right: Epsilon (top); Delta (bottom).

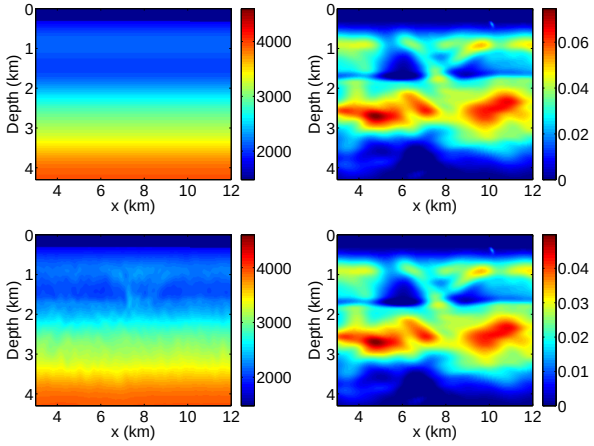

Figure 2: Left: Initial V_{P0} (top); Updated V_{P0} (bottom); Right: Updated epsilon (top); Updated delta (bottom).

The starting point for the velocity analysis is an isotropic 1D velocity model shown in figure 2. The model is constructed from a smoothed trace of the true velocity model. As discussed in the theory, we assume that the S-wave velocity is constant. Thus for migration we arbitrarily choose the values of the S-wave velocity to be 900 m/s over the whole model. And we couple the anisotropic parameters according to the fixed ratio of $\varepsilon = \frac{3}{2}\delta$.

The result of optimization on the parameters after 30 iterations are shown in figure 2. From this figure, we can see that the updated V_{P0} model is able to capture the main features of the upper 2.5 km of the true V_{P0} model, but fails to describe the deeper rotated structures. It is important to note that what we seek through the optimization are the background velocities, i.e., the smooth part of the velocity field, which is necessary to accurately explain the traveltimes. On the other hand, the estimated anisotropic parameters show a strong inprint of the P-wave velocity. This reveals a low sensitivity of the optimization towards the anisotropic parameters. The sensitivity of the anisotropic parameters could, in principle, be increased by a judicious change in parametrization, by a change in the acquisition geometry (longer surface offsets), or even by a different scaling of the data. However, this requires a sensitivity analysis, and is the subject of further research.

Figure 3 show a comparison of the RTM images produced with the initial 1D, WEMVA, and true model parameters. The initial image has large mispositionings and is poorly focused due to the inaccurate initial background velocities. These issues are largely fixed in the optimized migrated image, which is well focused and compares favourably with the image migrated with the true model. But there are some mispositionings (up to more than 50 meters) in the optimized image, in particular below 3 km depth.

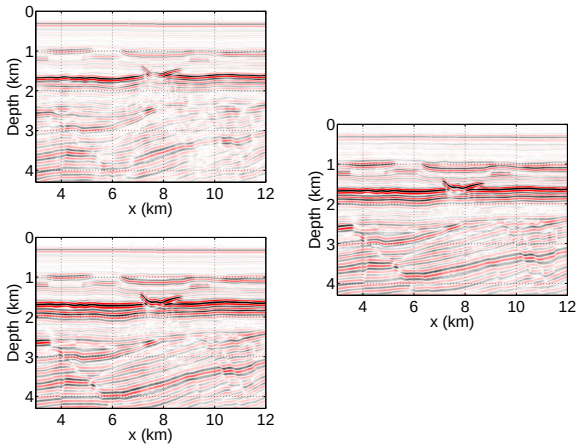

Figure 3: Left: Initial image (top); Optimized image (bottom). Right: True image.

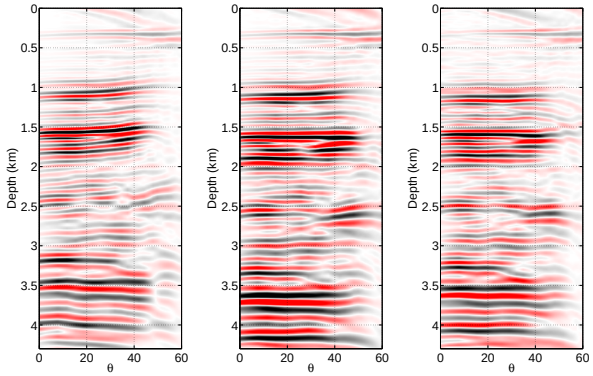

Figure 4: Angle gathers at position 8 km. Left: Initial 1D isotropic model ; Middle: WEMVA model. Right: True model.

Figure 4 shows a comparison of angle gathers extracted from the RTM images produced with the 1D initial isotropic model, the WEMVA model, and the true model. The angle gathers are

computed from the respective RTM image volumes using a subsurface offset to angle mapping (Biondi and Symes, 2004). The angle gathers provide a clearer way to quality control the estimated parameters. From this figure we can see that, in spite of the poor estimates of the anisotropic parameters, the optimization does a good job in flattening the angle gathers.

Overall, these results suggest that optimizing the focusing of subsurface offset CIGs produced by depth migration of surface seismic data might not be sufficient to constrain a unique anisotropic model. Due to this inherent non-uniqueness, the solution of the optimization leads to a final image that is well focused, but incorrectly positioned.

Field data example

In the next example we apply the method on a real dataset taken over the Snorre field offshore Norway. The data is originally a 3D marine dataset, from which we extract a 2D line. The geometry of the data consists of a line with minimum offset of 150 meters and maximum offset of 5 kilometers. The data processing included multiple removal, and muting of direct wave, wide-angle reflections and refractions. The maximum frequency of the data was filtered down to 30 Hz, so that a coarse grid of 20 by 20 meters could be used for modeling and migration.

The initial model for the optimization is shown in figure 5. It consists in an isotropic 1D model created by smoothing a well log of the vertical slowness.

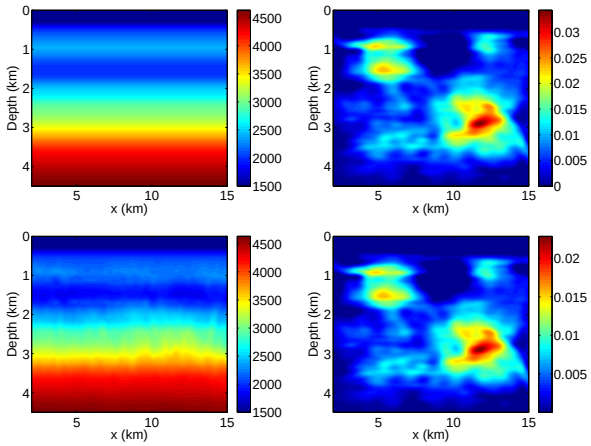

Figure 5: Left: Initial V_{P0} (top); Updated V_{P0} (bottom); Right: Updated epsilon (top); Updated delta (bottom).

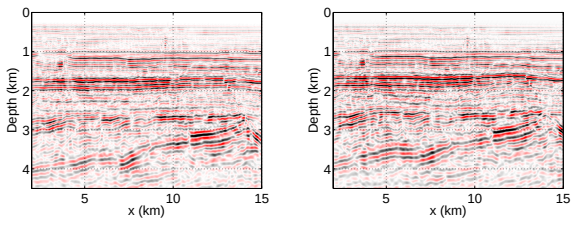

Figure 6: Left: Initial image. Right: Final image after 30 iterations.

The optimization is set to run for 30 iterations. The resultant estimated parameters are shown in figures 5. Notice that in this case the estimated anisotropic parameters, albeit small (less than 0.04 for ϵ and less than 0.03 for δ), are relatively independent from V_{P0}.

The migrated images computed with the initial and updated models are shown in figure 6, while figure 7 shows a comparison on selected angle gathers. We can see that optimization clearly improves the focusing of the RTM image and flattens the angle gathers. However, as in the synthetic data example, there is some uncertainty about the positioning of the reflectors in the final image.

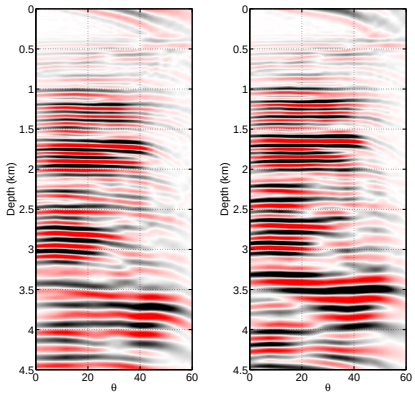

Figure 7: Angle gathers at position 8 km. Left: Initial 1D isotropic model ; Right: WEMVA model.

CONCLUSION

Results on synthetic and real field data show that our method provides an automatic and fast way of improving the quality of the depth migrated image.

In spite of the reduction of the model space to only two parameters, the optimization was dominated strongly by the P-wave velocity along the symmetry axis (V_{P0}). This reflects the low sensitivity of this type of optimization towards anisotropy. As a result, images are mispositioned in depth. Further research is necessary to make the method more sensitive to anisotropy, allowing more information to be extracted from surface seismic data.

The high computational cost is currently limiting the application of the method to 2D and low frequency datasets. Results could be further improved by adding more frequencies and the whole 3D dataset.

ACKNOWLEDGMENTS

We acknowledge the partners in the Snorre license, Statoil ASA, Petoro, ExxonMobil E&P Norway, Idemitsu Petroleum Norge, RWE, Dea Norge, Total E&P Norge and Core Energi AS for permission to publish the results.

REFERENCES

Alkhalifah, T., 2000, An acoustic wave equation for anisotropic media: Geophysics, **65**, 1239–1250.

Biondi, B., and W. W. Symes, 2004, Angle-domain common-image gathers for migration velocity analysis by wavefield-continuation imaging: Geophysics, **69**, 1283–1298.

Chavent, G., 2009, Non-linear least squares for inverse problems: Theoretical foundations and step-by-step guide for applications: Springer.

Chavent, G., and C. A. Jacewitz, 1995, Determination of background velocities by multiple migration fitting: Geophysics, **60**, 476–490.

Claerbout, J. F., 1971, Toward a unified theory of reflector mapping: Geophysics, **36**, 467–481.

Ikelle, L. T., and L. Amundsen, 2005, Introduction to petroleum seismology: Society of exploration geophysicists.

Lisitsa, V., and D. Vishnevskiy, 2010, Lebedev scheme for the numerical simulation of wave propagation in 3d anisotropic elasticity: Geophysical Prospecting, **58**, 619–635.

Rickett, J. E., and P. C. Sava, 2002, Offset and angle-domain common image-point gathers for shot-profile migration: Geophysics, **67**, 883–889.

Sava, P., and B. Biondi, 2004, Wave-equation migration velocity analysis. I. theory: Geophysical Prospecting, **52**, 593–606.

Shen, P., and W. W. Symes, 2008, Automatic velocity analysis via shot profile migration: Geophysics, **73**, 49–59.

Symes, W. W., and J. J. Carazzone, 1991, Velocity inversion by differential semblance optimization: Geophysics, **5**, 654–663.

Tarantola, A., 1984, Inversion of seismic reflection data in the acoustic approximation: Geophysics, **49**, 1259–1266.

———, 2005, Inverse problem theory and methods for model parameter etimation: SIAM (Society of Industrial and Applied Mathematics).

Thomsen, L., 1986, Weak elastic anisotropy: Geophysics, **51**, 1954–1966.

Weibull, W. W., and B. Arntsen, 2011, Reverse time migration velocity analsysis: Presented at the 73th EAGE Conference & Exhibition, European Association of Geoscientists and Engineers.